Geomorphology 375 (2021) 107550

Contents lists available at ScienceDirect

Geomorphology

journal homepage: www.elsevier.com/locate/geomorph

Patterns in river channel sinuosity of the Meuse, Roer and Rhine rivers in the Lower Rhine Embayment rift-system, are they tectonically forced?

H.A.G. Woolderink [a,*], K.M. Cohen [b], C. Kasse [a], M.G. Kleinhans [b], R.T. Van Balen [a,c]

[a] Vrije Universiteit Amsterdam, Faculty of Science, Earth and Climate Cluster, De Boelelaan 1085, Amsterdam 1081, HV, the Netherlands
[b] Department of Physical Geography, Faculty of Geosciences, Utrecht University, 3508, TC, Utrecht, the Netherlands
[c] TNO Geological Survey of the Netherlands, PO-Box 80015, Utrecht 3508, TA, the Netherlands

ARTICLE INFO

Article history:
Received 9 September 2020
Received in revised form 26 November 2020
Accepted 27 November 2020
Available online 3 December 2020

Keywords:
Sinuosity
Tectonics
Faulting
Rivers

ABSTRACT

The tectonic and fluvial setting of the Rhine-Meuse river system in the Lower Rhine Embayment rift system is exceptionally well known. The 19th century, pre-regulation river courses of three rivers are used to study a postulated sinuosity response to faulting. The fault-perpendicular Meuse River shows patterns of sinuosity changes at different spatial scales. The large-scale (>5 km) sinuosity changes are related mainly to the faulting-induced changes of the subsurface lithology, determining the bed and bank characteristics. However, at a smaller scale, some fault-related channel sinuosity anomalies are observed. The fault-parallel Roer River shows sinuosity changes related to a normal, non-tectonic longitudinal gradient change. Sinuosity patterns of the Rhine River are predominantly related to lithological differences and reduced incision rates. Sinuosity can thus be an indicator of tectonic motions, but gradient, subsurface lithology and river bank composition determine sinuosity as well. Therefore, a sinuosity change is no proof for fault activity. On the other hand, the absence of a sinuosity change does not imply inactivity of a fault at geological time-scales.

1. Introduction

The effect of tectonic vertical motions on (alluvial) river response has been a matter of interest over the past decades (Burnett and Schumm 1983; Ouchi 1985; Leeder and Alexander 1987; Holbrook and Schumm 1999; Marple and Talwani 2000, Buratto et al., 2003; Jain and Sinha 2005; Holbrook et al. 2006; Aswathy et al. 2008; Taha and Anderson 2008; Petrovszki and Timar, 2010, Arcos 2012; Lahiri and Sinha 2012; Mack et al. 2012; Whitney and Hengesh 2015). One of the commonly observed effects is a change in sinuosity. A sinuosity change is a means for the river to maintain a constant channel gradient. Via changes in the amount and size of the individual meander loops, the river channel is presumed to dynamically alter its channel length in such a way that the channel gradient remains unchanged despite the tectonic tilting (Holbrook and Schumm 1999). The sinuosity response to active faulting depends on the relation between the sense of movement and the flow direction. A normal fault with the hanging wall in the downstream direction (i.e. downstepping in downstream direction) will enhance the fluvial gradient and, as a result, an increased sinuosity will occur at the fault trace. In contrast, a normal fault that is downstepping in upstream direction may lead to a reduced gradient and, hence, sinuosity (Ouchi 1985; Holbrook and Schumm 1999). Both physical scale experiments and numerous field examples show that an increase of valley floor gradient results in increased sinuosity of the river channel or vice versa (Adams, 1980; Schumm and Harvey, 1985; Ouchi 1985; Gomez and Marron, 1991; Schumm et al. 1994; Smith et al. 1997; Holbrook and Schumm 1999; Schumm et al., 2002; Timár, 2003; Zámolyi et al., 2010; Petrovszki and Timár, 2010; Petrovszki et al. 2012). Most of the studies on the effects of tectonic vertical motions and river response show that sinuosity changes provide a means, as a geomorphic indicator, to identify active deformation from fluvial stratigraphic and -morphologic archives, which can be of large value for earthquake studies as demonstrated by Holbrook et al. (2006).

Sinuosity changes in meandering rivers, however, depend on many more factors than structural controls alone such as changes in discharge regime, erodibility of the river banks and channel bed, balance of bed load vs. suspended load, groundwater seepage and dominant mode of meander cut-off (chute or neck) (Baker 1978; Schumm 1963; Dade 2000; Van Balen et al. 2008; Stouthamer et al., 2011; Kleinhans and van den Berg, 2011; Pierik et al. 2017; Candel et al. 2020). Therefore, in the absence of independent constraints for tectonics, the attribution of observed sinuosity changes to either tectonic or other controlling factors is challenging. Moreover, case studies that do use sinuosity changes as indications of differential tectonic control are often restricted to the analyses of motions of fault-bounded blocks at the reach scale (Burnett 1982; Burnett and Schumm 1983; Jorgensen 1990; Jain and Sinha 2005; Lahiri and Sinha, 2012). Alternations in sinuosity, however,

* Corresponding author.
E-mail address: h.woolderink@vu.nl (H.A.G. Woolderink).

https://doi.org/10.1016/j.geomorph.2020.107550

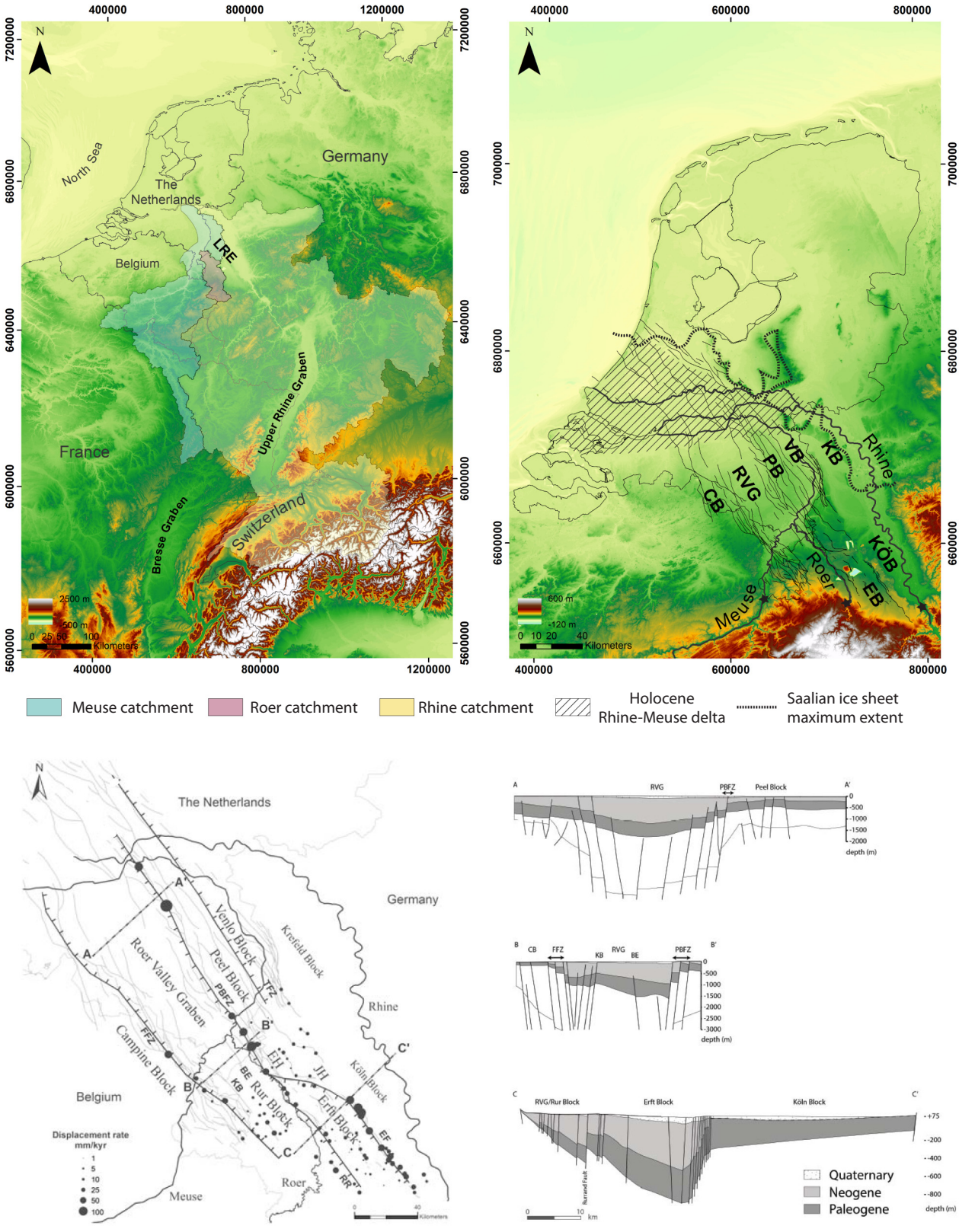

Fig. 1. The Lower Rhine Embayment (LRE) as part of the European Cenozoic rift system. The Meuse, Roer and Rhine rivers flow through the LRE. The Meuse crosses the rift system, the Roer parallels the Roer Valley Graben (RVG) and the Rhine occupies the rift margin. Tectonic displacements are the highest along the north-eastern boundary faults of the Roer Valley Graben (RVG) and Erft Block (EB). Displacement rates are adapted from Gold et al. (2017), Cohen (2003), Van Balen et al. (2019), Michon and Van Balen et al. (2005), Van den Berg et al. (2002), Houtgast et al. (2005) (after Woolderink et al. 2019).

can also be induced across fault zones at the sub-reach scale (i.e. just upstream vs. just downstream a fault trace). These more local responses to individual active faults may occur superimposed on regional-scale block-wise tilting caused by the tectonic structure at large. These aspects of scale complicate attributing sinuosity changes to tectonic controls and quantifying them against non-tectonic variations even further. The aim of this study is to investigate the possible role of tectonics (at multiple scales) as a forcing factor on river channel sinuosity. In this study we combine the well-known tectonic and sedimentary setting of three rivers (Meuse, Roer and Rhine) in the rift system of the Lower Rhine Embayment in NW Europe (SE Netherlands and adjacent Belgium and Germany) with morphometric sinuosity analyses of their pre-regulation courses (i.e. 19th cy). The rivers have diverse positions in the active rift system (i.e. transverse and lateral [Fig. 1 and section 2]) and, for the Meuse and Roer rivers, the displacement history of the faults in their courses are well-known from independent data. Moreover, variations in river bed and bank characteristics over the course of the rivers, which determine sinuosity as well, are also well known. The Lower Rhine Embayment rift system, therefore, provides a natural laboratory to unravel tectonically-forced responses of channel sinuosity from other forcing factors for rivers that are subjected to various degrees of faulting, both at the scale of fault-bounded blocks (> 5 km) and fault zones. The Meuse (transverse) and Roer (lateral) rivers are used to study the effect(s) of tectonic faulting on river sinuosity. The results of these rivers will help interpret sinuosity changes of the Rhine River as possible geomorphic indicators of (active) faulting at the rift margin (Fig. 1).

2. Fluvial and tectonic setting

2.1. Present-day characteristics of the Meuse, Roer and Rhine rivers

The Meuse River is a circa 900 km long rainfed river that has its headwaters in northeastern France (Fig. 1). The Meuse then flows along the rims of the Paris Basin and crosses the Ardennes Massif before it enters the tectonic system of this study at Eijsden (Fig. 1). The Meuse River crosses multiple fault zones of the Lower Rhine Embayment (LRE). Because it crosses the main graben of the rift system (i.e. the Roer Valley Graben [RVG]), rather than following it, its geomorphology (floodplain width, flanking terrace flights) is substantially affected by differential tectonics (Fig. 1 [Van den Broek and Maarleveld 1963; Van den Berg 1996; Huisink 1998, Woolderink et al. 2019). The Meuse enters its Holocene deltaic reaches where it turns westward in the central Netherlands (Fig. 1). The present-day mean annual discharge is circa 250 m^3/s and its bankfull discharge is approximately equal to mean annual flood, which is around 1500 m^3/s at Maaseik (Belgium; Table 1). The catchment size of the Meuse river system is 33,000 km^2. Gradients of the Meuse valley range between ~60 and 10 cm/km on average. The adaption length of the backwater curve lies between 7.5 and 52.5 km. The adaption length represents the upstream length up to which the effects of a downstream perturbation can propagate, which is an important factor when considering the effects of faulting on river morphodynamics.

The Roer River is the main tributary of the Meuse River in the study area, and has a catchment size of circa 2354 km^2. The Roer has it source in the Hautes Fagnes (Belgium) and has a length of 165 km. In the upstream ~85 km bedrock is dominant as it flows through the uplifting Eifel region. The downstream alluvial reach, circa 80 km, flows through the subsiding RVG (Fig. 1). The Roer enters the RVG at Düren and flows parallel to the direction of the graben and fault zones (Fig. 1). The mean annual discharge of the Roer River is ~21.8 m^3/s (at Stah, Germany) and discharge varies between 8 and 124 m^3/s (LANUV, n.d.; Table 1). Valley gradient varies between circa 230 and 90 cm/km and the adaption lengths of the backwater curves range between 0.8 and 2.9 km.

The Rhine River is the largest river passing through the rift system. It has a length of 1230 km and flows from the Alps in Switzerland, through Germany and the Netherlands to the North Sea (Fig. 1). The Rhine river is a snowmelt and rainfed river and its catchment is circa 185.000 km^2. The Rhine River enters the Lower Rhine Embayment at Bonn and takes a north westerly course along the eastern margin of the tectonic system, avoiding the rift system depocentres (Fig. 1). The river enters its deltaic reach in the Dutch-German border region. The mean annual discharge is around 2200 m^3/s at Rees (Germany [Erkens 2009]) and the mean annual flood discharge is ~6500 m^3/s. The adaption length for the backwater effect is around 29 km (Table 1) and valley gradient average lies between 35 and 20 cm/km.

2.2. Tectonic structure and depositional record

The Lower Rhine Embayment (LRE) forms the northern segment of the European Cenozoic Rift System (ECRIS). The ECRIS spans from the North Sea to the Mediterranean and also includes the Eger Graben (Czech Republic), Leinegraben (Germany), the Bresse, Limagne, Saône grabens, gulf of Lyon (France) and the Valencia Trough (Spain [Ziegler 1992]). The Roer Valley Rift System (RVRS) is part of the LRE (Fig. 1). The LRE is situated in the southern Netherlands and adjacent parts of Belgium and Germany (Fig. 1). The RVRS developed upon Palaeozoic to Mesozoic fault structures and has been reactivated multiple times in both reverse and normal faulting modes (Geluk et al. 1994; Van Balen et al. 2019). The last extension phase, which is still ongoing, started during the Late Oligocene. This extension can be related to the (ongoing) stresses exerted by the Alpine orogeny on its forelands (Ziegler 1992). The tectonic evolution of the LRE has been studied extensively (Fig. 1 [Ahorner 1962; Klostermann 1983; Zagwijn 1989; Schirmer 1990; Ziegler 1992, 1994; Geluk et al. 1994; Van den Berg 1996; Houtgast and Van Balen 2000; Houtgast et al. 2002; Cohen et al., 2002; Schäfer and Siehl 2002; Michon et al. 2003; Van Balen et al. 2005; Kemna 2005; Westerhoff et al. 2008]). The horst-graben structure of the LRE consist of asymmetric (half) grabens and symmetric (full) grabens (Fig. 1[Schäfer et al. 2005; Michon and Van Balen, 2005; Westerhoff et al. 2008]). The main fault zones of the LRE have a NW-SE orientation (Fig. 1). The most important grabens in the LRE are the Erft Block (EB) and the Roer Valley Graben (RVG)/Rur Block (RB) respectively. The RVG is bounded by the relatively uplifting Campine Block (CB) in the south and the Peel Block (PB) in the north (Van

Table 1
Main river characteristics of the gravel and sand reaches of the Meuse, Roer and Rhine rivers.

	Meuse Gravel	Meuse Sand	Roer Gravel	Roer Sand	Rhine Gravel
Qflood (M3\S)	1500		85		6500
Width (m)	125	150	40	30	425
Depth (m)	4.5	5.3	1.9	2.6	7.3
Width/depth	27.8	28.6	21.1	11.5	58.2
Gradient Valley (m/km)	0.6	0.1	2.3	0.9	0.35–0.20
Grainsize (m)	0.02–0.04	0.0005–0.001	0.04	0.0005–0.001	0.015–0.02
Sinuosity range	1.07–2.77	1.03–3.39	1.05–1.42	1.17–2.20	1.03–1.93
Shields number	0.05	0.40	0.06	1.61	0.06
Adaption length backwater effect (km)	7.5	52.5	0.8	2.9	29.2

Balen et al. 2005; Westerhoff et al. 2008). The upstream part of the CB consist of relatively cohesive Cretaceous and Paleogene limestone (hard) rocks. A transition to unconsolidated sands occurs near Maastricht. The shallow subsurface of the RVG consist mainly of relatively coarse-grained (older) Rhine-Meuse deposits. The PB is characterized by (cohesive) fine marine and coastal deposits of Miocene age. The Venlo Block (VB) consist predominantly of fluvial sediments (Woolderink et al. 2018 and references herein). The fault systems also continue in the subsurface of the Rhine-Meuse delta (Cohen et al., 2002), but are not considered a direct control to Late Holocene deltaic river reaches and hence these are left out of our sinuosity analysis.

The LRE has a general northwest tilting direction, which is a result of subsidence in the North Sea Basin (Kooi et al. 1991, 1998) and the Quaternary uplift of the Rhenish Shield (Van Balen et al. 2000; Demoulin and Hallot 2009). A secondary tilt direction to the northeast was observed for the tectonic blocks of the RVRS, based on lithostratigraphic mapping of the basin fill (Van Balen et al. 2000). A superimposed regional-scale, glacio-isostatic northward tilting component is reckoned to have been in play in the youngest 20,000 years (Kiden et al. 2002; Cohen 2003; Busschers et al. 2007; Hijma et al. 2009), owing to the near-field peripheral position of the region to land ice masses (forebulge collapse). However, the subsidence due to isostatic movements becomes insignificant during the past few thousand years compared to the tectonic component (Kiden et al. 2002).

The NE-SW directed extension led to a maximum of circa 1200–1500 m of subsidence in the RVG since the Late Oligocene (Geluk et al. 1994; Van Balen et al. 2005; Schäfer et al. 2005; Kemna 2005; Schokker et al. 2005; Westerhoff et al. 2008). An overview of the displacement rates of the (main) fault zones of the LRE is shown in Fig. 1. The highest displacement rates, and maximum sediment accumulation, occurs along the north-eastern boundary faults of the RVG and EB (Ahorner 1962; Schäfer et al. 1996; Camelbeeck and Meghraoui 1998; Van den Berg et al. 2002; Houtgast et al. 2002; Michon and Van Balen, 2005; Gold et al., 2017; Woolderink et al. 2019).

The Feldbiss Fault Zone (FFZ) separates the RVG from the CB in the south, while the Peel Boundary Fault Zone (PBFZ) forms the boundary between the RVG and PB in the north (Fig. 1). The river Meuse at present traverses these faults, and has had such a course since ~300.000 years ago (Van den Berg 1996; Houtgast et al. 2002; Schokker et al., 2007). The FFZ is downstepping in the flow direction of the Meuse River, while the PBFZ is downstepping in upstream direction. Both the FFZ and PBFZ reach to the surface and are visible as fault scarps and in seismic and geo-electric profiles (DINOloket, 2019; Paulissen, 1985; Vanneste et al., 2002). The Koningsbosch (KB) and Beegden (BE) faults delineate a small horst within the subsiding RVG (Fig. 1). The KB fault reaches up to the Meuse river bed, is visible on shallow river seismic sections and on geo-electric profiles, and is downstepping in upstream direction (Demco, 1998; Tigrek et al., 2000). The BE fault has not been surveyed and it is unknown whether this fault reaches up to the river bed. According to borehole data (DINOloket, 2019), the fault seems not to have affected deposits of the Meuse River of the last ~300.000 years and there is no morphological expression of the BE. The BE normal fault steps down in downstream direction. Present-day and Holocene displacement rates of the KB and BE faults are unknown.

In the southeastern part of the LRE, the PBFZ splits into the Rur (RR) and Erft (EFZ) fault zones. The Rur Fault (RR) separates the RVG/RB from the EB. The Köln Block (KÖB) forms the hanging wall in the eastern part of the LRE, where it is separated from the EB by the Ville horst and Erft Fault Zone (EFZ) (Fig. 1 [Schäfer et al. 2005]). The Ville horst continues to the northwest into the Jackerather and Erkelenz horsts respectively (cf. Ahorner 1962). The continuation of these horst structures form the Peel Block in the Netherlands (Fig. 1). The PB is bordered by the Venlo Block (VB) that lies to the north (Fig. 1).

The VB and PB are separated by the Tegelen Fault Zone (TFZ). The TFZ consist of three faults that are all downstepping in downstream direction of the Meuse (Fig. 1). The faults reach up to the river bed according to shallow-seismic river profiles (Tigrek et al., 2000). The displacement rates of the faults have not been constrained in the study area. However, since these faults have no morphologic expression, their average rates should be less than those of the historically seismically active FFZ and the PBFZ. An estimation of displacement rates, between ~0.02 mm/yr (±0.01) and 0.11 (±0.02), of the TFZ more to the north was given by Cohen et al. (2002).

In the northeast a relatively high block, the Krefeld Block (KB), borders the subsiding VB area (Geluk et al. 1994). The shallow subsurface of the KB consist mainly of Pleistocene fluvial gravel and sand of the Rhine River (NRW 2019).

The LRE main fault zones are seismically active with the 1756 Düren (Mw 5.7) and 1992 Roermond (Mw 5.4) earthquakes as the most significant examples (Geluk et al. 1994; Camelbeeck et al. 2007). Paleoseismological data from trench studies over the PBFZ and FFZ shows that fault displacement has been episodic, especially during the Lateglacial period (Vanneste and Verbeeck 2001; Vanneste et al. 2001; Van den Berg et al. 2002; Camelbeek et al., 2007; Vandenberghe et al., 2009; Vanneste et al. 2018; Van Balen et al. 2019).

3. Methods

Both the longitudinal profiles and sinuosity calculations are based on the early 19th century courses of the Meuse, Roer and Rhine rivers as these courses pre-date most regulations (e.g. dykes, weirs, groins, channelization) of the rivers. The Meuse channel was digitized from the georeferenced Topografische en Militaire kaart van het Koninkrijk der Nederlanden 1850–1864 (Kadaster 1850). The river channels of the Roer and Rhine were derived from the Tranchot Maps 1801–1828.

3.1. Longitudinal profiles

In a GIS, points were placed along the digitized 19th cy. river channels with a spacing of 100 m. For each of the points the height was extracted from a 1 m (horizontal) resolution contemporary Digital Elevation Model [AHN2, n.d.; Land NRW, n.d.]. Hereafter the height was plotted against the distance along the river channel (Fig. 2). A considerable bandwidth of height points is generated by this method due to (gravel/sand) mining, inclusion of water-bodies and presence of anthropogenic (infra) structures along certain stretches of the rivers. This is especially the case for the Meuse River in the RVG (Fig. 2). Therefore, median values were established, where each median is calculated over a sliding window across neighbouring elevation points, for the longitudinal channel profile of each of the rivers. The window size was determined by incrementally increasing the window size until the inflection point, after which an increase in window size did not contribute to a smoother profile anymore. The window sizes used for the Meuse, Roer and Rhine are 101, 51 and 161 points (or 10, 5 and 16 km) respectively. By using this method the median elevation values become dependent on the sinuosity of the river channel, which varies spatially over the longitudinal profile of the rivers.

Valley gradients were calculated by $S_v = P * S_c$, where S_c = channel slope and P is the sinuosity, in order to retrieve them separately for each sinuosity zone. Hereafter the potential specific stream power ω_{pv} (W/m^2), which is a parameter for the potential maximum of the available flow energy for a river stretch with a sinuosity of 1 (Kleinhans and van den Berg, 2011), was calculated for each sinuosity reach of the rivers. It is defined as $\omega_{pv} = \frac{\rho g Q S_v}{W_r}$, where ρ = water density (kg m^{-3}), g = gravitational acceleration (m s^{-2}), Q = channel forming discharge (m^3/s), S_v = valley slope (−) and W_r = reference channel width. The channel reference width is predicted by $W_r = \alpha\sqrt{Q}$ where $\alpha = 4.7$ for sand ($D_{50} < 2$ mm) and 3.0 for gravel ($D_{50} > 2$ mm) reaches of the rivers (Van den Berg 1995; Kleinhans and van den Berg, 2011). The calculation of streampower per sinuosity-reach used in this study is a relatively crude approach and is hence mostly suited to indicate relatively large-scale variations in

streampower over the length of the longitudinal river profiles. However, this sinuosity-reach approach is very well-suited to compare the reach-specific streampower and sinuosity of the river channel to fault locations, which is the focus of this study.

3.2. Sinuosity

Sinuosity is defined as the ratio of channel length over valley length. Sinuosity can be computed at the largest scale, using the valley length corresponding to the whole river stretch, as well as to shorter parts of river valley stretches. Therefore, sinuosity is analysed and presented as a function of length-scale in this study (e.g. Lancaster and Bras 2002; Van Balen et al. 2008). The average sinuosity for the whole range of potential lengths was calculated, (zero to fifteen kilometres), to determine the most suitable length-scale. The minimum length resulting in the maximum average sinuosity was selected as lengths above this minimum value have no significant contribution to sinuosity (Appendix A). The length scales used for the Meuse, Roer and Rhine sinuosity calculations are respectively 7.5, 3 and 12,5 km (Appendix A).

4. Results and interpretation

4.1. Longitudinal profiles

The Meuse River shows a distinct break in the gradient of the longitudinal profile, and associated peak in gradient change, around 15 km along the river channel (Fig. 2). Relatively high changes in gradient occur around the FFZ (i.e. HH, GF, FF), KB, BE and just in front of the PBFZ I (Fig. 2). However, the overall channel gradient over the CB and RVG remains relatively stable around 0.35 m/km. A peak in the change of gradient occurs at ~105 km along the river channel. The average channel gradient over the PB and VB reduces to ~8 cm/km (90–175 km).

The Roer River has a concave river profile with a gradual change in gradient around 46 km along the river channel profile (Fig. 2). Here the channel gradient reduces from ~204 cm/km in the upstream part to ~70 cm/km in the reach downstream of the concavity (Fig. 2). The change in gradient reduces in the downstream direction (Fig. 2). The change in gradient of the Roer River is relatively peaked compared to the Meuse and Rhine rivers.

The channel gradient of the Rhine River between ~8 and 85 km is ~19 cm/km (Fig. 2). Between ~85 and 135 km this gradient steepens to ~24 cm/km. The gradient of the channel changes relatively abruptly around 158 km, this is, however, due to an anomaly in the Digital Elevation Model and has no natural cause. From 135 to 208 km the gradient of the Rhine channel reduces to ~13 cm/km.

4.2. Sinuosity patterns

4.2.1. Meuse

The early 19th century course of the Meuse can be visually subdivided into three sinuosity zones, labelled M1-M3 (Fig. 3).

In sinuosity reach M1 the Meuse River is relatively straight with sinuosity values of ~1.07–1.13. In the next downstream stretch, M2, the sinuosity is larger, ranging between 1.19 and 2.76 (Fig. 3). Despite the increase in sinuosity from zone M1 to M2, the coarseness of the bed load (gravel) and the discharge remain constant. However, the erodibility of the bed and banks is different in stretch M1. Here the subsurface consists of relatively cohesive Cretaceous and Paleogene limestone, while in the upstream part of zone M2 the bed and banks consist of unconsolidated sands (https://www.dinoloket.nl, 2019). The relatively hard limestone likely reduces vertical erosion and lateral movement and hence sinuosity of the river channel in zone M1 (Figs. 3 and 4).

The peak in change of gradient around 15 km along the river channel (Fig. 4) coincides with the lithological transition (from limestone to sands) of the subsurface. This increases erodibility of bed and banks downstream of the lithological transition and hence a larger gradient is observed in zone M2 (Fig. 4). This results in an enhanced lateral displacement and, consequently, a sinuosity increase (Figs. 3 and 4). More downstream, in the RVG the lithology changes to coarse-grained gravel and sands of older Rhine-Meuse fluvial deposits that are still relatively easily reworked and, therefore, promote lateral dynamics of the river and thus sinuosity.

Zone M3 is characterized by sinuosity values between 1.08 and 1.30, which shows that the river in this reach is rather straight (Fig. 3). This is

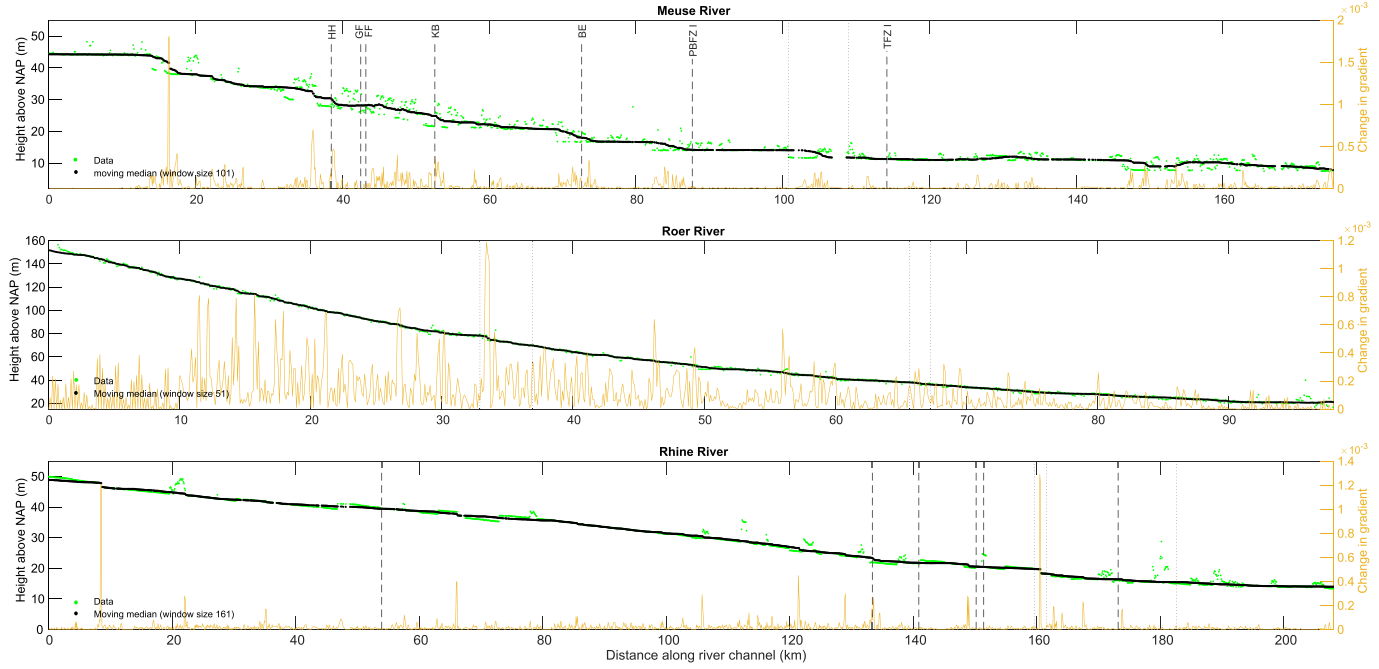

Fig. 2. Early 19th century longitudinal river channel profiles of the Meuse, Roer and Rhine rivers. Dashed lines represent (semi) perpendicular crossing by the river channels of the (postulated) faults of the Lower Rhine Embayment. Dotted lines indicate a parallel course of the river channel and the fault zone. NAP is the dutch ordnance datum.

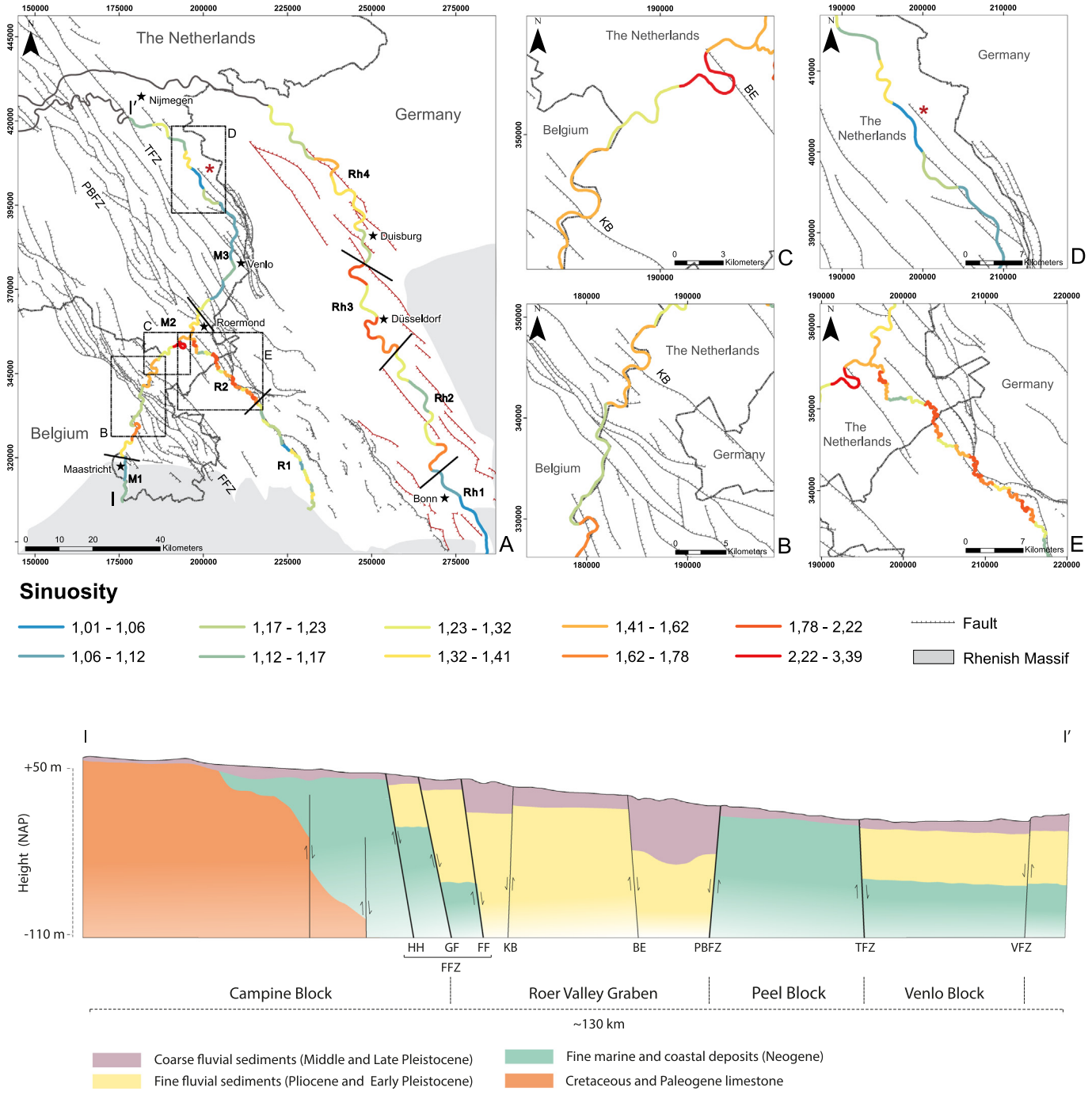

Fig. 3. A: Sinuosity analysis (per reach) of the early 19th century Meuse, Roer and Rhine rivers. The presence of the red coloured fault zones is uncertain. The transition from Cretaceous and Paleogene limestone to unconsolidated sands roughly coincides with the division between M1 and M2. B: Sinuosity changes of the Meuse over the Feldbiss and Koningsbosch fault zones. C: Sinuosity changes of the Meuse over the downstepping in upstream direction Koningsbosch and downstepping in downstream direction Beegden fault zones. D: Meanders (yellow) in zone M3 with a relatively high sinuosity that occur above strike-extrapolated strands of the TFZ I (indicated by the red asterisk). E: High-sinuosity reach R2 of the Roer River. Transect I-I′ shows a schematic representation of the lithology of the (faulted) shallow subsurface along the longitudinal profile of the Meuse River in the LRE.

in line with a reduction of the gradient and associated stream powers in this reach (Fig. 4). However, the change in subsurface lithology over the PBFZ I is an additional factor to be taken into account for the sinuosity change. In the upstream part of zone M3, on the PB, the subsurface lithology consists of cohesive Miocene, Pliocene and Early Pleistocene fine-grained sands and clays (Woolderink et al. 2018 and references herein). This reduces bank erosion and, hence, lateral movement and sinuosity. Moreover, bank height increases over the PB and VB due to ongoing incision during the Holocene. These factors hamper lateral dynamics of the river channel. Vertical incision thus prevails over lateral movement, resulting in a low-sinuosity channel of the Meuse River in zone M3 (Fig. 4; [Woolderink et al. 2018]).

4.2.2. Roer

The early 19th century course of the Roer River can be divided into two reaches based on the sinuosity of the river channel (Fig. 3). Zone R1 is characterized by relatively low sinuosity values between 1.04 and 1.40. Sinuosity increases in zone R2 with values ranging between

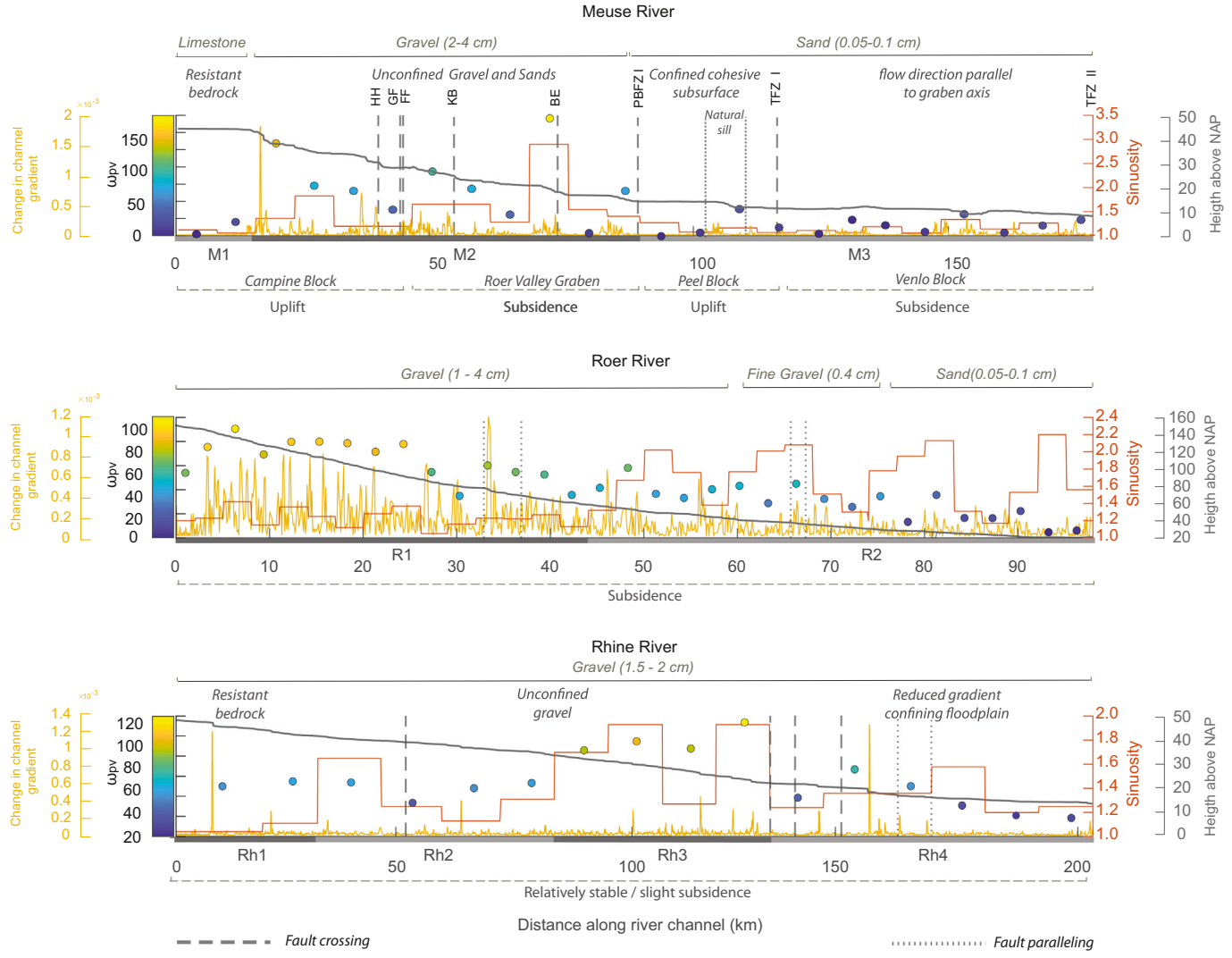

Fig. 4. Sinuosity, potential specific stream power and (change) in channel gradient along the longitudinal channel profiles and sinuosity zones of the early 19th century Meuse, Roer and Rhine rivers. Dashed lines represent (semi) perpendicular crossing by the river channels of (postulated) faults of the Lower Rhine Embayment. Dotted lines indicate a parallel course of the river channel and the fault zone.

~1.20 and 2.20 (Fig. 3). The increase in sinuosity values at ~46 km along the river channel of the Roer (Fig. 3) coincides with a decrease in gradient from ~204 cm/km in zone R1 to ~70 cm/km in zone R2 (Fig. 4). A reduced gradient results in a reduced potential specific stream power (Fig. 4) and, therefore, in a shift from a chute-dominated meandering pattern to a scroll-bar dominated meandering river pattern (cf. Kleinhans and van den Berg, 2011 [Fig. 5D]). Frequent chute cut offs will result in a decrease in sinuosity of the channel, while increased scroll-bar formation enhances lateral migration and sinuosity. The threshold between chute-dominated to scroll-bar dominated meandering for the Roer River lies around a ω_{pv} value of ~60 (Fig. 5D). Although exact grainsize measurements were not available for the upstream part of the Roer River, a general classification of so-called "Grobkies and Mittelkies", corresponding to a grainsize of 6.3 10^{-3}–6.3 10^{-2} m, was derived for the bedload in this reach (NRW 2019). For this grainsize range our threshold in stream power between scroll-bar dominated and chute-dominated meandering for the Roer River falls within the empirically derived threshold shown by Kleinhans and van den Berg, 2011 [Appendix B]).

The negative correlation between stream power and sinuosity for the Roer River is shown by Figs. 4 and 5F. It is striking that sinuosity reaches of the Roer River that are outside the trend can be explained by a change in lithology (Fig. 5F). Furthermore, the sinuosity zone in which the Roer River "crosses" fault zones of the LRE parallelly, fits the trend of sinuosity versus stream power, indicating that the sinuosity of the Roer River is not influenced by tectonics (Fig. 5F). The results for the Roer River show that sinuosity is dependant on other factors than tectonics (i.e. grain-size, chute and neck cut-off, bank strength and height [Baker 1978; Schumm 1963; Dade 2000; Kleinhans and van den Berg, 2011; Candel et al. 2020]).

4.2.3. Rhine

The early 19th century course of the Rhine River can be subdivided into four sinuosity zones (Fig. 3 zones Rh1-Rh4). Zone Rh1 is relatively straight with sinuosity values between 1.04 and 1.10 (Fig. 3). This low sinuosity is not the result of a reduced gradient, which is relatively high in this upstream reach (with corresponding high streampowers [Fig. 4]), or a change in discharge. Bedrock lithology, however, offers an explanation for the relatively straight river channel in zone Rh1 compared to a more sinuous channel in zone Rh2 (Figs. 3 and 4). The relatively resistant Palaeozoic bedrock of the Rhenish Massif hampers lateral movement of the Rhine River and, therefore, sinuosity in reach Rh1. Within zone Rh2 sinuosity increases to values ranging between 1.13 and 1.60

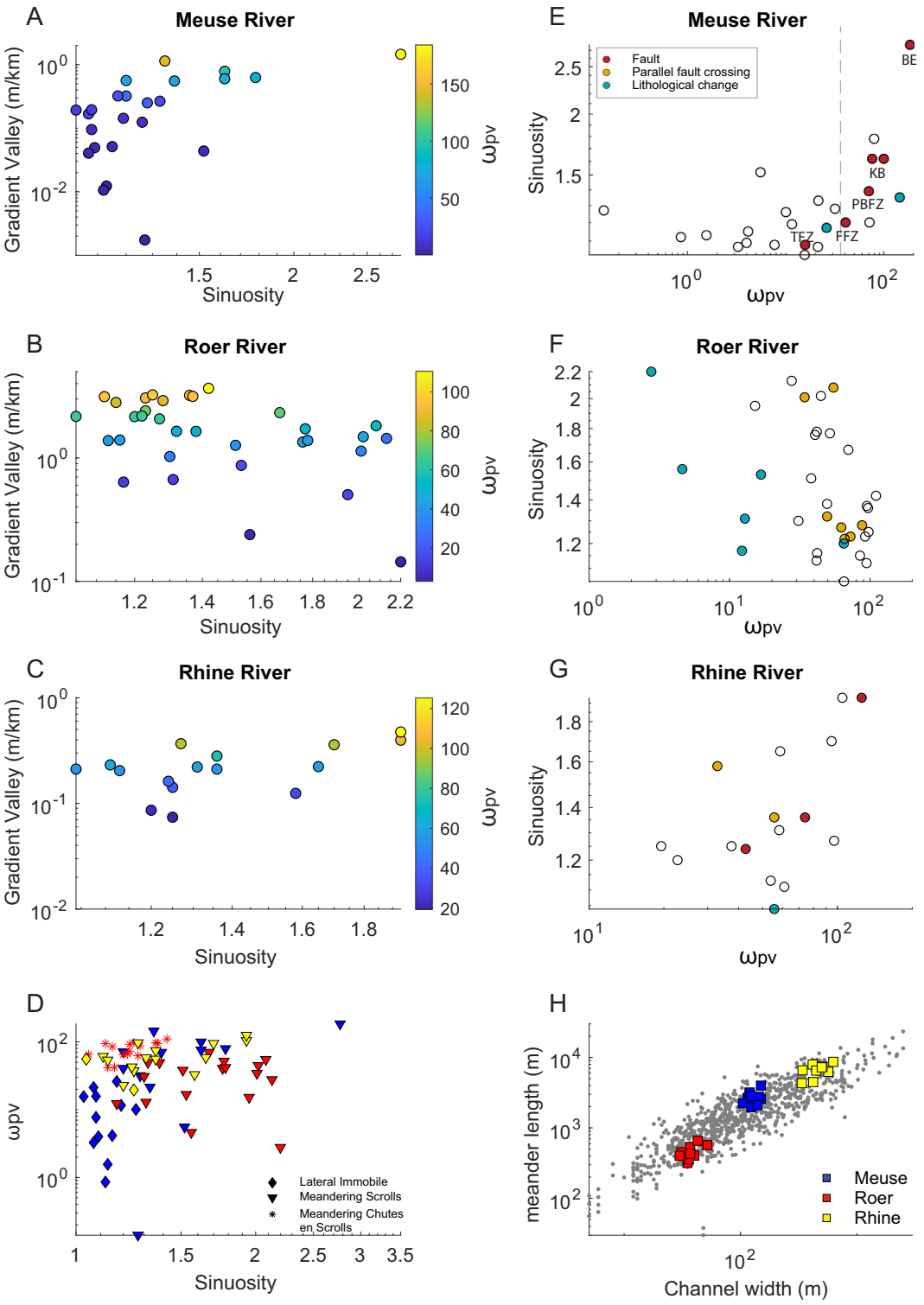

Fig. 5. A–C: Valley gradient vs sinuosity for the Meuse, Roer and Rhine, respectively. The circles represent the sinuosity reaches of the rivers. The Meuse river shows no clear relationship between valley gradient and sinuosity. The Roer has a negative correlation while the Rhine shows a positive correlation between sinuosity and gradient of the valley D: Potential specific stream power versus sinuosity for the different fluvial planforms of the Meuse, Roer and Rhine. E–G: Sinuosity versus potential specific stream power for the Meuse, Roer and Rhine, respectively. Open circles represent null conditions. The legend for the Meuse applies to the panels of the Roer and Rhine as well. The Meuse shows no clear relationship, while the Roer and Rhine show a negative and positive correlation respectively. Sinuosity zones that coincide with fault locations, parallel fault crossings or lithological changes of the subsurface are indicated by colour. H: Relation between meander length and channel width of the meandering reaches of the Meuse, Roer and Rhine rivers. Grey points are adapted from Leuven et al. (2018).

(Fig. 3). The subsurface lithology changes from the Palaeozoic slates in zone Rh1 to Quaternary sand and gravel of older Rhine deposits in zone Rh2 (NRW 2019). This change in subsurface lithology, together with the transition from a confined to a more unconfined setting, results in a sinuosity increase in zone Rh2 due to more easily lateral erodible banks.

Zone Rh3 is the part of the Rhine with the highest sinuosity values; these vary between 1.26 and 1.91 (Fig. 3). The erodibility of the subsurface does not change between zone Rh2 and Rh3, as the river channel remains in the alluvial sediments of older Rhine deposits (NRW 2019). There is, however, a slight increase in gradient in zone Rh3, to ~24 cm/km, and associated stream powers (Figs. 2 and 4). This increase in gradient is, most likely, the cause of the higher sinuosity of zone Rh3. The increase in sinuosity between zone Rh2 and Rh3 does not coincide with any known fault structure of the LRE (Fig. 3). In fact, the most sinuous part of the river channel in Rh3 flows more or less parallel to the strike of the known fault zones of the rift system (Fig. 3), making a fault related forcing unlikely.

Attributing changes in sinuosity in the Lower Rhine, e.g. into and out of reach Rh3, to tectonic controls at this stage of research can only be speculative. In zone Rh3 the Rhine course is positioned relatively closer to the LRE margin and the flanking Rhenish Massif and outside the Quaternary depocentre (which lies somewhat to the west). Such could explain why both the sinuosity and gradient increases in zone Rh3 (Figs. 1 and 3). If so, the gradient increase is the result of touching the very margin of the rift system in the area, and not so much controlled by neotectonically active faults, but by inherited structures from before Oligocene-Miocene rift system reactivation.

Downstream, in zone Rh4, sinuosity decreases to between 1.23 and 1.57 (Fig. 3). The reduced sinuosity in zone Rh4 (compared to zone Rh3) coincides with a decreased gradient of the longitudinal profile in this zone (Figs. 2 and 4). Such a reduced gradient might be caused by active tectonics (Schumm et al. 2002) and the transition coincides with postulated fault locations (Ahorner 1962). It is, however, unlikely that this reduced gradient is a result of active tectonics because the faults do not have a surface expression in the (older) floodplain(s) of the Rhine River. Moreover, remnants of slightly older Rhine channels are highly sinuous (Erkens et al. 2011; Cohen et al. 2012). A more likely cause for the reduced gradient is a reduced incision rate (as proposed by Erkens et al. 2011), which is caused by aggradation of fines in this reach, similar to the deltaic reaches downstream. Moreover, the transition between zone Rh3 and Rh4 coincides with the maximum extent of the Saalian ice-sheet (Fig. 1), resulting in a local depocentre and hence reduced gradients in zone Rh4.

5. Discussion

5.1. Large-scale sinuosity patterns

The analyses of sinuosity changes suggests that large-scale sinuosity characteristics of the Meuse River are closely related to the location of faults, but not to faulting. The sinuosity of the Meuse River is indirectly (or passively) controlled by faulting as the faulted subsurface of the LRE causes differences in channel bed lithology, gradient and bank height along the river profile. This is shown in Fig. 4 which shows the stream power plotted over the longitudinal channel profile. The high-sinuosity zone M2 coincides with a relatively high gradient, while zone M3 has low-sinuosity values due to the flattened gradient and cohesive and fine-grained lithology in the relatively uplifting PB and VB (Fig. 4). The same passive tectonic control was also observed for the previously investigated fluvial terraces of the Meuse river (Woolderink et al. 2018). A reach-specific tectonic control on river sinuosity was, for instance, also observed in the Mississippi River (Schumm et al. 1994) and Baghmati River (Jain and Sinha 2005). From this it could be concluded that a faulted subsurface influences the large-scale sinuosity patterns of alluvial rivers in active tectonic (rift) systems.

However, the Roer River shows that different sinuosity zones along a river can be the result of a concave river profile with associated changes in streampower and bedload grainsize, without tectonic forcing or faults along the longitudinal river profile (Fig. 4). For the Pannagon River (India) it was shown that the style and degree of river channel sinuosity also depends not solely on tectonics but on a number of other (geological) factors and riparian vegetation as well (Aswathy et al. 2008). Furthermore, the experiments by Schumm and Khan (1972) showed that sinuosity only increases with gradient up to a threshold, a further increase leads to a braided river pattern in which sinuosity is lower. The Roer River shows that it is not necessary to have a channel pattern shift to a braided style to accomplish a sinuosity decrease with increasing gradient, but that frequent chute cut-offs within the self-organized meandering domain lead to a similar result (Figs. 4 and 5B, D).

The sinuosity changes of the Rhine River, positioned at the rift-margin, also show large scale sinuosity patterns (Fig. 2). A trend of increasing sinuosity and gradient seems apparent for zone Rh3 in Fig. 4. This is supported by Fig. 5C and G that show a general positive trend between valley gradient/stream power and sinuosity (cf. Holbrook and Schumm 1999; Timár, 2003; Petrovszki et al. 2012), albeit for a certain range of valley gradient and stream power (i.e. in the meandering with scroll bar domain cf. Kleinhans and Van den Berg, 2011 [Appendix B]). Overall, the variations in river sinuosity of the early 19th century course of the Rhine River do not seem to be actively tectonically forced as sinuosity zones can be attributed to other causes such as inherited lithological differences, downstream reduced incision rates and changes in bank height and composition. Moreover, the sinuosity zones in which the river channel crosses fault zones fall within the positive trend that can be observed for the Rhine, indicating that sinuosity changes are not bounded to fault zones. Sinuosity is, therefore, not considered to be a valid indicator of tectonic activity for the Rhine River.

The above illustrates that an indirect relation between faulting, subsurface lithology and sinuosity exists for the Meuse river in the Lower Rhine Embayment rift system, but not for the Roer and Rhine rivers. Therefore, specific relations between faulting,valley slope and sinuosity cannot be generalized (cf. Kleinhans and van den Berg, 2011)

5.2. Local sinuosity anomalies at fault zones

A local change in sinuosity occurs in zone M2, around the Feldbiss Fault Zone (FFZ) (Figs. 3 and 4). Here sinuosity first decreases to ~1.2, when the Meuse river approaches the FFZ, after which sinuosity increases to ~1.6 when entering the RVG (Fig. 3). The FFZ consist of three faults that are downstepping in the downstream direction (e.g. Heerlerheide, Geleen and Felbiss faults). The faults of the FFZ are active and fault scarps occur on the late Middle Pleistocene terraces next to the Holocene floodplain (Houtgast et al. 2005; Camelbeeck et al. 2007). Relatively high changes in gradient occur around the FFZ (Figs. 2 and 4). A local sinuosity increase at fault-zone scale at the FFZ might thus be expected, in response to the downstepping normal faults and associated increase in gradient (Holbrook and Schumm 1999). Such an increase in sinuosity was evidenced for rivers in the Pannonian Basin and the Mississippi River (Schumm et al. 1994; Holbrook and Schumm 1999; Petrovszki et al. 2012). However, a sinuosity decrease is observed at the FFZ (Fig. 3).

The lack of a sinuosity increase around the FFZ implies that either the rate of faulting (and associated increase in gradient) is not high enough to force a sinuosity change, or that in-channel erosion and sedimentation has levelled height differences to such an extent that a sinuosity change was not established. Alternatively, a sinuosity decrease, as observed for the FFZ, can be explained by a gradient increase. The Roer River shows that higher gradients upstream lead to more chute cut-offs of the channel which reduces channel sinuosity (Fig. 4). This is considered as a likely cause for the relatively low-sinuosity reaches over the FFZ as local increased channel gradients are still observed in the channel profile and because the Meuse is near the threshold to a chute cut-off dominated meandering river (cf. Kleinhans and van den Berg, 2011 [Appendix B]) at the FFZ (Table 1). This is supported by remnants of phases of higher sinuosity and the presence of chute-channels in the adjacent floodplain at the FFZ.

A notable alignment of two relatively high-sinuosity meanders occurs along the Koningbosch Fault (KB) and the Beegden Fault (BE), which delineate a small horst within the RVG (Figs. 1 and 3C). A reduced sinuosity is expected at the KB fault due to its upstream directed down stepping (Fig. 1) and resulting decrease in gradient. An increase in sinuosity is expected at the BE fault (Fig. 1) because of an increase in gradient at a fault that is downstepping in downstream direction (Holbrook and Schumm 1999). There is no change in subsurface lithology over the KB fault which could account for the increased sinuosity at this fault zone. A local increase in channel gradient is, however, observed for the KB (Fig. 2). This might be the cause of the increased sinuosity of the KB fault, though this is the opposite of the expected sinuosity decrease from the downstepping in upstream direction of the KB fault. The sinuosity increase at the downstepping Beegden fault (BE) could imply that the fault reaches upon the river bed and is tectonically active. Alternatively, the high sinuosity might be the result of the confluence with the Roer River which would lead to a knickpoint and increased valley gradient and, hence, a larger sinuosity of the meandering Meuse in this area than both upstream and downstream (Fig. 3).

Sinuosity of the channel decreases over the PBFZ, which is downstepping in the upstream direction, when transitioning from the RVG to the PB (Fig. 3). However, the gradient, stream power and sinuosity remain relatively high up to the PBFZ (Figs. 3 and 4). This shows that the tectonic configuration of a fault-bounded horst exerts a substantially different form of forcing on river channels than dome-shaped warping (cf. Holbrook and Schumm 1999). In the latter, a sinuosity decrease is to be expected in front of the axis of uplift where the gradient decreases.

Uplift may expose more resistant substrates underneath otherwise alluvial rivers, resulting in channel profile anomalies (Holbrook and Schumm 1999). This is also observed for the Meuse River between ~100 and 110 km (Figs. 2 and 4). Here resistive layers of clay and lignite are locally exposed in the Meuse channel (causing a natural sill), leading to an increased gradient of the longitudinal profile (Figs. 2 and 4). This does, however, not mean that there is active deformation present at this location, but rather implies a passive tectonic control on the longitudinal profile. Our results, therefore, concur with Holbrook and Schumm (1999) who stated that such complexities and profile adjustments can rarely be used to indicate uplift without other evidence.

The faults of the TFZ I reach up to the river bed at the transition between the PB and VB, but no effect of fault displacement (i.e. an expected sinuosity increase) is noticeable in the channel gradient or the sinuosity (Figs. 2, 3 and 4). This implies that either no displacement has occurred along the TFZ I for, at least, the last two centuries or that slip rates were minor enough for the river channel to adjust to by in-channel erosion and sedimentation.

Two relatively high-sinuosity meanders occur in M3, but no fault is known at this location (Fig. 3D). However, the meanders occur above strike-extrapolated strands of the TFZ I, 6 km to the northwest, which could imply our current fault data base is incomplete (Fig. 3D, red asterisk).

A possible correlation between fault zones and sinuosity and stream power for the Meuse River can be observed from Fig. 5E. Almost all fault zones that reach upon the surface have a relatively high stream power. There is, however no relationship between stream power and sinuosity for the fault zones (Fig. 5E). Moreover, all the high stream power segments fall within large-scale sinuosity zone M2 (Figs. 3 and 4), which is characterized by a relatively high gradient and unconfined floodplain and gravel/sand lithology of the subsurface. This endorses our previous observation that the sinuosity of the Meuse river is influenced by fault-bounded blocks (Fig. 3), but that there is no uniform relation between fault zone scale vertical tectonic movements and sinuosity (Fig. 5E).

From the above it can be concluded that sinuosity change as an indicator of abrupt tectonic vertical motions along fault zones is not straightforward. Therefore, unless the different forcing factors can be unravelled by detailed morphometric analysis and a well constrained tectonic and sedimentary framework, (local) sinuosity anomalies should be interpreted as an indicator of possible tectonic deformation at best. In this our results coincide with Schumm (1986) and Holbrook and Schumm (1999) who mention that alternative explanations must be addressed before sinuosity change can be considered valid as an indicator of tectonic deformation. Moreover, the rate at which fluvial morphodynamics occur might be much higher than that of tectonic faulting. This can lead to reworking of fluvial response(s) to faulting by subsequent river dynamics. It is, therefore, important to be aware of such transient river response when interpreting the geomorphological and sedimentological record for fault related sinuosity anomalies.

6. Conclusions

The effects of tectonic vertical m.ent on the Meuse (crossing the faults), Roer (parallel to the faults) and Rhine (rift margin) rivers have been investigated and the following can be concluded:

- The sinuosity of the early 19th century course of the Meuse river is (indirectly) controlled by tectonics on a block-scale as this determines the large-scale differences in valley gradient and subsurface lithology, and hence the erodibility of the river bed and banks.
- Downstream sinuosity increases along the Roer River are the result of a decreasing gradient along the concave river profile and associated change from a chute-dominated to scroll-bar dominated meandering system.
- The early 19th century course of the Rhine River does not reveal any tectonic controls or fault zone activity. Changes in sinuosity are mostly related to lithological differences, reduced incision rates and changes in bank height and composition.
- The relation between fault motions, river gradient and sinuosity is not straightforward as sinuosity is also controlled by (o.a.) river bed and bank characteristics, intrinsic fluvial dynamics, meandering style and because sinuosity varies over time.
- Sinuosity change as an indicator of tectonic motions can only be used in combination with a well-known tectonic and sedimentary framework. The absence of a sinuosity change does not imply inactivity of the fault at geological time-scales, nor is a deviating sinuosity value proof of fault activity.

Supplementary data to this article can be found online at https://doi.org/10.1016/j.geomorph.2020.107550.

Declaration of competing interest

The authors confirm that there are no known conflicts of interest associated with this publication and there has been no financial support for this work that could have influenced its outcome.

Acknowledgements

This research is part of a PhD project "Reconstruction and Modelling of the Meuse and Rhine River. Sinuosity Response to Faulting in the Roer Valley Rift System" funded by Netherlands Organisation for Scientific Research (NWO; project nr. 821.01.011). We would like to thank John Holbrook, Gábor Timár and an anonymous reviewer for their constructive comments and review that helped improve this manuscript.

References

Adams, J., 1980. Active tilting of the United States midcontinent: geodetic and geomorphic evidence. Geology 9, 442–446.

Ahorner, L., 1962. Untersuchungen zur quartären Bruchtektonik der Niederrheinischen Bucht. Quaternary Science Journal 13 (1), 24–105.

Arcos, M.E.M., 2012. A Holocene sedimentary record of tectonically influenced reduced channel mobility, Skokomish River delta, Washington State, USA. Geomorphology 177, 93–107.

Aswathy, M.V., Vijith, H., Satheesh, R., 2008. Factors influencing the sinuosity of Pannagon River, Kottayam, Kerala, India: an assessment using remote sensing and GIS. Environ. Monit. Assess. 138 (1–3), 173–180.
Baker, V., 1978. Adjustment of fluvial systems to climate and source terrain in tropical and subtropical environments. In: Miall, A.D. (Ed.), Fluvial Sedimentology. 5. Memoir-Canadian Society of Petroleum Geologists, pp. 211–230.
Burnett, A.W., 1982. Alluvial Stream Response to Neotectonics in the Lower Mississippi Valley. Doctoral dissertation, Colorado State University.
Burnett, A.W., Schumm, S.A., 1983. Alluvial-river response to neotectonic deformation in Louisiana and Mississippi. Science 222 (4619), 49–50.
Burrato, P., Ciucci, F., Valensise, G., 2003. An inventory of river anomalies in the Po Plain, Northern Italy: evidence for active blind thrust faulting. Ann. Geophys. 46 (5), 865–882.
Busschers, F.S., Kasse, C., Van Balen, R.T., Vandenberghe, J., Cohen, K.M., Weerts, H.J.T., Wallinga, J., Johns, C., Cleveringa, P., Bunnik, F.P.M., 2007. Late Pleistocene evolution of the Rhine-Meuse system in the southern North Sea basin: imprints of climate change, sea-level oscillation and glacio-isostacy. Quat. Sci. Rev. 26 (25–28), 3216–3248.
Camelbeeck, T., Meghraoui, M., 1998. Geological and geophysical evidence for large palaeo-earthquakes with surface faulting in the Roer Graben (northwest Europe). Geophys. J. Int. 132 (2), 347–362. https://doi.org/10.1046/j.1365-246x.1998.00428.x.
Camelbeeck, T., Vanneste, K., Alexandre, P., Verbeeck, K., Petermans, T., Rosset, P., Mazzotti, S., 2007. Relevance of active faulting and seismicity studies to assessments of long-term earthquake activity and maximum magnitude in intraplate Northwest Europe, between the Lower Rhine Embayment and the North Sea. In: Stein, S., Mazzotti, S. (Eds.), Continental Intraplate Earthquakes: Science. Hazard, and Policy Issues, Special Paper 425. Geological Society of America, Boulder, Colorado, pp. 193–224.
Candel, J.H.J., Kleinhans, M.G., Makaske, B., Wallinga, J., 2020. Predicting river channel pattern based on stream power, bed material and bank strength. Progress in Physical Geography: Earth and Environment. 1 (26), 1–26. https://doi.org/10.1177/0309133320948831.
Cohen, K.M., 2003. Differential Subsidence within a Coastal Prism: Late-Glacial-Holocene Tectonics in the Rhine-Meuse Delta, the Netherlands. Doctoral dissertation, Utrecht University.
Cohen, K.M., Stouthamer, E., Berendsen, H.J.A., 2002. Fluvial deposits as a record for late Quaternary neotectonic activity in the Rhine-Meuse delta, the Netherlands. Netherlands Journal of Geosciences - Geologie en Mijnbouw 81, 389–405.
Cohen, K.M., Stouthamer, E., Pierik, H.J., Geurts, A.H., 2012. Rhine-Meuse Delta Studies' Digital Basemap for Delta Evolution and palaeogeography. Department of Physical Geography, UNIVERSITEIT Utrecht, Digital Dataset, DANS, (November 10, 2016). doi:10.17026/dans-x7g-sjtw.
Dade, W., 2000. Grain size, sediment transport and alluvial channel pattern. Geomorphology 35, 119–126.
Demco, 1998. Geo-elektrische metingen op de Grensmaas. Report R980110A. Projektbureau Maaswerken, Maastricht, The Netherlands, pp. 1–13.
Demoulin, A., Hallot, E., 2009. Shape and amount of the Quaternary uplift of the western Rhenish shield and the Ardennes (western Europe). Tectonophysics 474 (3–4), 696–708.
Erkens, G., 2009. Sediment Dynamics in the Rhine Catchment: Quantification of Fluvial Response to Climate Change and Human Impact. Doctoral dissertation, Utrecht University.
Erkens, G., Hoffmann, T., Gerlach, R., Klostermann, J., 2011. Complex fluvial response to late glacial and Holocene allogenic forcing in the lower Rhine valley (Germany). Quat. Sci. Rev. 30, 611–627.
Geluk, M.C., Duin, E.T., Dusar, M., Rijkers, R.H.B., Van den Berg, M.W., Van Rooijen, P., 1994. Stratigraphy and tectonics of the Roer Valley Graben. Geol. Mijnb. 73, 129.
Gold, R.D., Friedrich, A., Kübler, S., Salamon, M., 2017. Apparent Late Quaternary Fault-Slip Rate Increase in the Southern Lower Rhine Graben, Central Europe. Bulletin of the Seismological Society of America 107 (2), 563–580.
Gomez, B., Marron, D.C., 1991. Neotectonic effects on sinuosity and channel migration, Belle Fourche River, western South Dakota. Earth Surface Processes and Landforms 16, 227–235.
Hijma, M.P., Cohen, K.M., Hoffmann, G., Van der Spek, A.J.F., Stouthamer, E., 2009. From river valley to estuary: the evolution of the Rhine mouth in the early to middle Holocene (western Netherlands, Rhine-Meuse delta). Netherlands Journal of Geosciences - Geologie en Mijnbouw 88, 13–53.
Holbrook, J., Schumm, S.A., 1999. Geomorphic and sedimentary response of rivers to tectonic deformation: a brief review and critique of a tool for recognizing subtle epeirogenic deformation in modern and ancient settings. Tectonophysics 305 (1–3), 287–306.
Holbrook, J., Autin, W.J., Rittenour, T.M., Marshak, S., Goble, R.J., 2006. Stratigraphic evidence for millennial-scale temporal clustering of earthquakes on a continental-interior fault: Holocene Mississippi River floodplain deposits, New Madrid seismic zone, USA. Tectonophysics 420 (3–4), 431–454.
Houtgast, R.F., Van Balen, R.T., 2000. Neotectonics of the Roer Valley rift system, the Netherlands. Glob. Planet. Chang. 27 (1–4), 131–146.
Houtgast, R.F., Van Balen, R.T., Bouwer, L.M., Brand, G.B.M., Brijker, J.M., 2002. Late Quaternary activity of the Feldbiss Fault Zone, Roer Valley Rift System, the Netherlands, based on displaced fluvial terrace fragments. Tectonophysics 352, 295–315. https://doi.org/10.1016/S0040-1951(02)00219-6.
Houtgast, R.F., Van Balen, R.T., Kasse, C., 2005. Late Quaternary evolution of the Feldbiss Fault (Roer Valley Rift System, the Netherlands) based on trenching, and its potential relation to glacial unloading. Quat. Sci. Rev. 24 (3–4), 489–508.
AHN 2, n.d.. http://www.ahn.nl/index.html (accessed 1 February 2020).
Data en Informatie van Nederlandse Ondergrond (DINOloket), (2019). DINOloket, https://www.dinoloket.nl. (accessed November 11, 2019).
Huisink, M., 1998. Tectonic versus climatic controls on the River Maas dynamics during the Late Glacial. In: Baker, V.R., Gregory, K.J. (Eds.), Benito, G. John Wiley and Sons, Palaeohydrology and Environmental Change, pp. 99–109.
Jain, V., Sinha, R., 2005. Response of active tectonics on the alluvial Baghmati River, Himalayan foreland basin, eastern India. Geomorphology 70 (3–4), 339–356.
Jorgensen, D.W., 1990. Adjustment of Alluvial River Morphology and Process to Localized Active Tectonics. Doctoral dissertation, Colorado State University.
Kadaster, 1850. Topografische Militaire Kaart van het Koninkrijk der Nederlanden. 1850. TMK. DANS. https://doi.org/10.17026/dans-zrx-wz6e.
Kemna, H.A., 2005. Pliocene and Lower Pleistocene Stratigraphy in the Lower Rhine Embayment, Germany, Doctoral dissertation. Universität Köln.
Kiden, P., Denys, L., Johnston, P., 2002. Late Quaternary sea-level change and isostatic and tectonic land movements along the Belgian–Dutch North Sea coast: geological data and model results. J. Quat. Sci. 17 (5–6), 535–546.
Kleinhans, M.G., van den Berg, J.H., 2011. River channel and bar patterns explained and predicted by an empirical and a physics-based method. Earth Surf. Process. Landf. 36 (6), 721–738.
Klostermann, J., 1983. Die Geologie der Venloer Scholle (Niederrhein). Geologisches Landesamt Nordrhein-Westfalen, Krefeld.
Kooi, H., Hettema, M., Cloetingh, S., 1991. Lithospheric dynamics and the rapid Pliocene-Quaternary subsidence phase in the southern North Sea basin. Tectonophysics 192 (3–4), 245–259.
Kooi, H., Johnston, P., Lambeck, K., Smither, C., Molendijk, R., 1998. Geological causes of recent (~100 yr) vertical land movement in the Netherlands. Tectonophysics 299 (4), 297–316.
Lahiri, S.K., Sinha, R., 2012. Tectonic controls on the morphodynamics of the Brahmaputra River system in the upper Assam valley, India. Geomorphology 169, 74–85.
Lancaster, S.T., Bras, R.L., 2002. A simple model of river meandering and its comparison to natural channels. Hydrol. Process. 16 (1), 1–26.
Land NRW, (n.d.). Datenlizenz Deutschland-Namensnennung-Version 2.0 (www.govdata. de/dl-de/by-2-0). https://www.opengeodata.nrw.de/produkte/geobasis/dgm/ (accessed 1 February 2020).
Leeder, M.R., Alexander, J.A.N., 1987. The origin and tectonic significance of asymmetrical meander-belts. Sedimentology 34 (2), 217–226.
Leuven, J.R., van Maanen, B., Lexmond, B.R., van der Hoek, B.V., Spruijt, M.J., Kleinhans, M. G., 2018. Dimensions of fluvial-tidal meanders: are they disproportionally large? Geology 46 (10), 923–926.
Mack, G.H., Leeder, M., Perez-Arlucea, M., Durr, M., 2012. Tectonic and climatic controls on Holocene channel migration, incision and terrace formation by the Rio Grande in the Palomas half graben, southern Rio Grande rift, USA. Sedimentology 58 (5), 1065–1086.
Marple, R.T., Talwani, P., 2000. Evidence for a buried fault system in the Coastal Plain of the Carolinas and Virginia—implications for neotectonics in the southeastern United States. Geol. Soc. Am. Bull. 112 (2), 200–220.
Michon, L., Van Balen, R.T., 2005. Characterization and quantification of active faulting in the Roer valley rift system based on high precision digital elevation models. Quat. Sci. Rev. 24 (3–4), 455–472.
Michon, L., Van Balen, R.T., Merle, O., Pagnier, H., 2003. The Cenozoic evolution of the Roer Valley Rift System integrated at a European scale. Tectonophysics 367, 101–126. https://doi.org/10.1016/S0040-1951(03)00132-X.
NRW, 2019. IS GK 100 (WMS)– Datensatz. Datenlizenz Deutschland-Namensnennung-Version 2.0 (www.govdata.de/dl-de/by-2-0). https://www.geoportal.nrw/themenkarten (accessed 15 Oktober 2019).
Ouchi, S., 1985. Response of alluvial rivers to slow active tectonic movement. Geol. Soc. Am. Bull. 96 (4), 504–515.
Paulissen, E., Vandenberghe, J., Gullentops, F., 1985. The Feldbiss fault in the Maas valley bottom (Limburg, Belgium). Geol. Mijnb. 64, 79–87.
Petrovszki, J., Timár, G., 2010. Channel sinuosity of the Körös River system, Hungary/Romania, as possible indicator of the neotectonic activity. Geomorphology 122 (3–4), 223–230.
Petrovszki, J., Székely, B., Timár, G., 2012. A systematic overview of the coincidences of river sinuosity changes and tectonically active structures in the Pannonian Basin. Glob. Planet. Chang. 98, 109–121.
Pierik, H.J., Stouthamer, E., Cohen, K.M., 2017. Natural levee evolution in the Rhine-Meuse delta, the Netherlands, during the first millennium CE. Geomorphology 295, 215–234.
Schäfer, A., Siehl, A., 2002. Preface: Rift tectonics and syngenetic sedimentation-the Cenozoic Lower Rhine Basin and related structures. Neth. J. Geosci. 81 (2), 145–147. https://doi.org/10.1017/S001677460002237X.
Schäfer, A., Hilger, D., Gross, G., Von der Hocht, F., 1996. Cyclic sedimentation in Tertiary Lower-Rhine Basin (Germany)—the 'Liegendrücken' of the brown-coal open-cast Fortuna mine. Sedimentary Geology, 103(3–4), 229–247. doi:https://doi.org/10.1016/0037- 0738(95)00091-7.
Schäfer, A., Utescher, T., Klett, M., Valdivia-Manchego, M., 2005. The Cenozoic Lower Rhine Basin–rifting, sedimentation, and cyclic stratigraphy. Int. J. Earth Sci. 94 (4), 621–639. https://doi.org/10.1007/s00531-005-0499-7.
Schirmer, W., 1990. Rheingeschichte zwischen Mosel und Maas. Deuqua-Führer 1, 295.
Schokker, J., Cleveringa, P., Murray, A.S., Wallinga, J., Westerhoff, W.E., 2005. An OSL dated middle and Late Quaternary sedimentary record in the Roer Valley Graben (southeastern Netherlands). Quaternary Science Reviews 24 (20−21), 2243–2264. https://doi.org/10.1016/j.quascirev.2005.01.010.
Schokker, J., Weerts, H.J.T., Westerhoff, W.E., Berendsen, H.J.A., Otter, C.D., 2007. Introduction of the Boxtel Formation and implications for the Quaternary lithostratigraphy of the Netherlands. Netherlands Journal of Geosciences/Geologie en Mijnbouw 86 (3).

Schumm, S.A., 1963. Sinuosity of alluvial rivers on the Great Plains. Geol. Soc. Am. Bull. 74 (9), 1089–1100.
Schumm, S.A., 1986. Alluvial river response to active tectonics. Active tectonics 80–94.
Schumm, S.A., Khan, H.R., 1972. Experimental study of channel patterns. Geol. Soc. Am. Bull. 83 (6), 1755–1770.
Schumm, S.A., Harvey, M.D., 1985. Preliminary geomorphic evaluation of the Sacramento River (Red Bluff to Butte Basin). Unpublished repot to Sacramento District. Corps of Engineers, p. 57.
Schumm, S.A., Rutherfurd, I.D., Brooks, J., 1994. Pre-cutoff morphology of the lower Mississippi River. In: Schumm, S.A., Winkley, B.R. (Eds.), The Variability of Large Alluvial Rivers. American Society of Civil Engineers Press, New York, pp. 13–44.
Schumm, S.A., Dumont, J.F., Holbrook, J.M., 2002. Active Tectonics and Alluvial Rivers. Cambridge University Press.
Smith, N.D., McCarthy, T.S., Ellery, W.N., Merry, C.L., Rüther, H., 1997. Avulsion and anastomosis in the panhandle region of the Okavango Fan, Botswana. Geomorphology 20, 49–65.
Stouthamer, E., Cohen, K.M., Gouw, M.J., 2011. Avulsion and its implications for fluvial-deltaic architecture: insights from the Holocene Rhine-Meuse delta. SEPM Spec. Publ 97, 215–232.
Taha, Z.P., Anderson, J.B., 2008. The influence of valley aggradation and listric normal faulting on styles of river avulsion: a case study of the Brazos River, Texas, USA. Geomorphology 95 (3–4), 429–448.
Tigrek, S., Kiden, P., Houtgast, R.F., Van Kuijk, J.M., 2000. A high-resolution seismic survey on the river Maas. Petrophysics meets Geophysics, 6–8 November, Paris.
Timár, G., 2003. Controls on channel sinuosity changes: a case study of the Tisza River, the Great Hungarian Plain. Quat. Sci. Rev. 22 (20), 2199–2207.
Van Balen, R.T., Houtgast, R.F., Van der Wateren, F.M., Vandenberghe, J., Bogaart, P.W., 2000. Sediment budget and tectonic evolution of the Meuse catchment in the Ardennes and the Roer Valley Rift System. Glob. Planet. Chang. 27, 113–129.
Van Balen, R.T., Houtgast, R.F., Cloetingh, S.A.P.L., 2005. Neotectonics of the Netherlands: a review. Quat. Sci. Rev. 24 (3–4), 439–454.
Van Balen, R.T., Kasse, C., De Moor, J., 2008. Impact of groundwater flow on meandering; example from the Geul River, the Netherlands. Earth Surf. Process. Landf. 33 (13), 2010–2028.
Van Balen, R.T., Bakker, M.A.J., Kasse, C., Wallinga, J., Woolderink, H.A.G., 2019. A late Glacial surface rupturing earthquake at the Peel Boundary fault zone, Roer Valley Rift System, the Netherlands. Quat. Sci. Rev. 218, 254–266.
Van den Berg, J., 1995. Prediction of alluvial channel pattern of perennial rivers. Geomorphology 12, 259–279.
Van den Berg, M., Vanneste, K., Dost, B., Lokhorst, A., Van Eijk, M., Verbeeck, K., 2002. Paleoseismic investigations along the Peel Boundary Fault: geological setting, site selection and trenching results. Neth. J. Geosci. 81 (1), 39–60. https://doi.org/10.1017/S0016774600020552.
Van den Berg, M.W., 1996. Fluvial Sequences of the Maas: A 10 Ma Record of Neotectonics and Climate Change at Various TimeScales. Doctoral dissertation, Landbouwuniversiteit Wageningen.
Van den Broek, J.M.M., Maarleveld, G.C., 1963. The late Pleistocene terrace deposits of the Meuse. Mededelingen Geologische Stichting NS 16, 13–24.
Vandenberghe, D., Vanneste, K., Verbeeck, K., Paulissen, E., Buylaert, J.P., De Corte, F., 2009. Late Weichselian and Holocene earthquake events along the Geleen fault in NE Belgium: OSL age constraints. Quat. Int. 199 (1–2), 56–74.
Vanneste, K., Verbeeck, K., 2001. Paleoseismological analysis of the Rurrand fault near Julich, Roer Valley graben, Germany: Coseismic or aseismic faulting history? Geol. Mijnb. 80 (3/4), 155–170.
Vanneste, K., Verbeeck, K., Camelbeeck, T., Paulissen, E., Meghraoui, M., Renardy, F., Jongmans, D., Frechen, M., 2001. Surface-rupturing history of the Bree fault scarp, Roer Valley graben: evidence for six events since the late Pleistocene. J. Seismol. 5 (3), 329–359.
Vanneste, K., Verbeeck, K., Camelbeeck, T., 2002. Exploring the Belgian Maas valley between Neeroeteren and Bichterweert for evidence of active faulting. Aardkundige Mededelingen 12, 5–8.
Vanneste, K., Camelbeeck, T., Verbeeck, K., Demoulin, A., 2018. Morphotectonics and past large earthquakes in Eastern Belgium. In: Demoulin, A. (Ed.), Landscapes and Landforms of Belgium and Luxembourg. World Geomorphological Landscapes. Springer, Cham, pp. 215–236 https://doi.org/10.1007/978-3-319-58239-9_13.
Westerhoff, W.E., Kemna, H.A., Boenigk, W., 2008. The confluence area of Rhine, Meuse, and Belgian rivers: Late Pliocene and Early Pleistocene fluvial history of the northern Lower Rhine Embayment. Netherlands Journal of Geosciences-Geologie en Mijnbouw 87 (1), 107.
Whitney, B.B., Hengesh, J.V., 2015. Geomorphological evidence for late Quaternary tectonic deformation of the Cape Region, coastal west Central Australia. Geomorphology 241, 160–174.
Woolderink, H.A.G., Kasse, C., Cohen, K.M., Hoek, W.Z. Van Balen, R.T., 2018. Spatial and temporal variations in river terrace formation, preservation, and morphology in the lower Meuse Valley, the Netherlands. Quat. Res. 91 (2), 548–569.
Woolderink, H.A.G., Kasse, C., Grooteman, L.P.A., Van Balen, R.T., 2019. Interplay between climatic, tectonic and anthropogenic forcing in the Lower Rhine Graben, the Roer River. Geomorphology 344, 25–45.
Zagwijn, W.H., 1989. The Netherlands during the Tertiary and the Quaternary: a case history of coastal lowland evolution. Geol. Mijnb. 68, 107–120.
Zámolyi, A., Székely, B., Draganits, E., Timár, G., 2010. Neotectonic control on river sinuosity at the western margin of the Little Hungarian Plain. Geomorphology 122 (3-4), 231–243.
Ziegler, P.A., 1992. European Cenozoic rift system. Geodynamics of rifting 1, 91–111.
Ziegler, P.A., 1994. Cenozoic rift system of western and Central-Europe, an overview. Geol. Mijnb. 73 (2–4), 99–127.